PERGAMON

Progress in Biophysics & Molecular Biology 74 (2000) 115–140

Progress in Biophysics & Molecular Biology

www.elsevier.com/locate/pbiomolbio

Review

Twisting and stretching single DNA molecules

Terence Strick[a,*], Jean-Francois Allemand[a,b], Vincent Croquette[a], David Bensimon[a]

[a] *LPS, ENS, UMR 8550 CNRS, 24 rue Lhomond, 75231 Paris Cedex 05, France*

[b] *Département de Chimie, ENS, UMR 8640 CNRS, 24 rue Lhomond, 75231 Paris, Cedex 05, France*

Abstract

The elastic properties of DNA are essential for its biological function. They control its bending and twisting as well as the induction of structural modifications in the molecule. These can affect its interaction with the cell machinery. The response of a single DNA molecule to a mechanical stress can be precisely determined in single-molecule experiments which give access to an accurate measurement of the elastic parameters of DNA.

Contents

*Corresponding author.

0079-6107/00/$ - see front matter
PII: S0079-6107(00)00018-3

1. Introduction

The past seven years have witnessed the emergence of a wealth of new techniques and tools for the study of single-molecule biophysics. Methods as diverse as optical and magnetic tweezers, microfibers and atomic force microscopy are now used in many labs to manipulate (displace, stretch or twist) single biomolecules (DNA, proteins, carbohydrates, etc.). In parallel optical methods based on fluorescence (by energy transfer or directly with evanescent wave, two-photons or confocal configurations) have also been developed to study biochemical processes at the single-molecule level. Currently, many groups are actively trying to combine both aspects, i.e. to visualize the displacement and activity of a single-molecule (myosin, RNA-polymerase, etc.) under stress.

In this paper we shall focus on the manipulation of single DNA molecules and on the measurement of their elastic properties in particular. After a brief review of the relevance of these properties to the biology of DNA, we shall describe the techniques involved in the manipulation of DNA. First, the anchoring of the molecule's ends to appropriate surfaces and the use of a meniscus to stretch and align a DNA molecule on a surface. This technique known as molecular combing has found many applications in the field of genomics. We shall then review various techniques for the manipulation of DNA and in particular the magnetic trap which allows one to both pull and twist a single-molecule. We will then present the various models used to describe DNA under tension and discuss their adequacy with the experimental results. The stretching of twisted DNA will be reviewed with an emphasis on the measurement of the torsional constant of the molecule and a description of the torque-induced structural phase transitions. Finally we shall review some of the experiments studying DNA/protein interactions at the single-molecule level.

DNA is one of the longest molecule in nature. A human chromosome for example is a few centimeters long. To squeeze such a lengthy molecule in a micron-size nucleus DNA is strongly bent and wrapped around histones, forming the bead on a string structure of chromatin, itself further compactified by extensive coiling. The bending and torsional properties of DNA (and chromatin) are therefore essential to an understanding of its compactification in the nucleus.

DNA is a polymer, i.e. a linear chain made of repeating structural units. These consist of a ribose-phosphate to which four different groups can be linked: adenine (A), guanine (G), cytosine (C) or thymine (T). DNA differs from most polymers in that it is formed by the winding around each other of two ribose-phosphate polymer chains (a DNA strand) locked by hydrogen bonding

between their complementary bases: adenine (guanine) on one strand with thymine (cytosine) on the other. This double helical structure prevents the relaxation of torsional stress by rotation about a single covalent bond as common with man-made polymers. Moreover, the stacking of the bases on top of each other confers unto DNA an unusually large flexional rigidity.

This structure also poses some formidable mechanical problems to the cellular machinery which has to read, transcribe and replicate the instructions of the genetic code buried inside the double helix. To make the code accessible to the DNA or RNA polymerase enzymes, the molecule has to be unwound and the two strands separated. Thus, as an RNA polymerase proceeds along the molecule the DNA upstream of the transcription complex is overwound, whereas downstream it is underwound (Liu and Wang, 1987). The regulation of the winding and torsional stresses involved in those processes is performed by a battery of enzymes known as topoisomerases (Wang et al., 1998). To study the function of these DNA-associated molecular motors one has to first understand the mechanical response of DNA under stress.

2. Single molecule micromanipulation

There are by now many new techniques to manipulate single molecules: optical (Simmons et al., 1996) or magnetic tweezers (Amblard et al., 1996; Gosse and Croquette, 1999) and traps (Smith et al., 1996; Strick et al., 1996), atomic force cantilevers (Florin et al., 1994), microfibers (Ishijima et al., 1991; Cluzel et al., 1996) and hydrodynamic drag (Smith et al. 1992). In all these techniques, a DNA molecule (but also a protein or some other polymer) is first anchored to a surface at one end and to a force sensor at the other. The force sensor is usually a trapped micron-sized bead or a cantilever whose displacements are used to measure the force, see Fig. 1. Different force range and measurement time scales are afforded by these techniques. Magnetic traps and microfibers further allow twisting of the molecule by rotating the magnets or the fibers where the bead is attached.

The upper bound for force measurements in micromanipulation experiments is the tensile strength of a covalent bound, on the order of $\mathrm{eV}/\mathring{A}$ or about 1000 pN (1 pN $= 10^{-12}$ N). The smallest measurable force is set by the Langevin force which is responsible for the Brownian motion of the sensor. Because of its random nature, the Langevin force is a noise density in force which is simply written as $f_n = \sqrt{4k_BT6\pi\eta r}$ (η is the viscosity of the medium, r is the radius of the particle). For a $1-\mu$m diameter bead in water, $f_n \sim 0.017\,\mathrm{pN}/\sqrt{\mathrm{Hz}}$. In between those two extremes lies the forces typical of the molecular scale, which are of order $k_BT/\mathrm{nm} \sim 4\,\mathrm{pN}$. This is roughly the stall force of a single-molecular motor such as myosin (4 pN; Finer et al., 1994) or RNA-polymerase (15–30 pN; Yin et al., 1995; Wang et al., 1998). It is also the typical force needed to unpair the DNA bases (about 15 pN; Essevaz-Roulet et al., 1997).

2.1. End-specific anchoring of DNA and molecular combing

The first step in any DNA manipulation experiment is to anchor the DNA (preferentially via its extremities) to appropriately treated surfaces. Many different methods have been developed to achieve specific DNA binding to surfaces. They have found useful applications, from gene mapping, sequencing and analysis (Chee et al., 1996) to the development of very sensitive

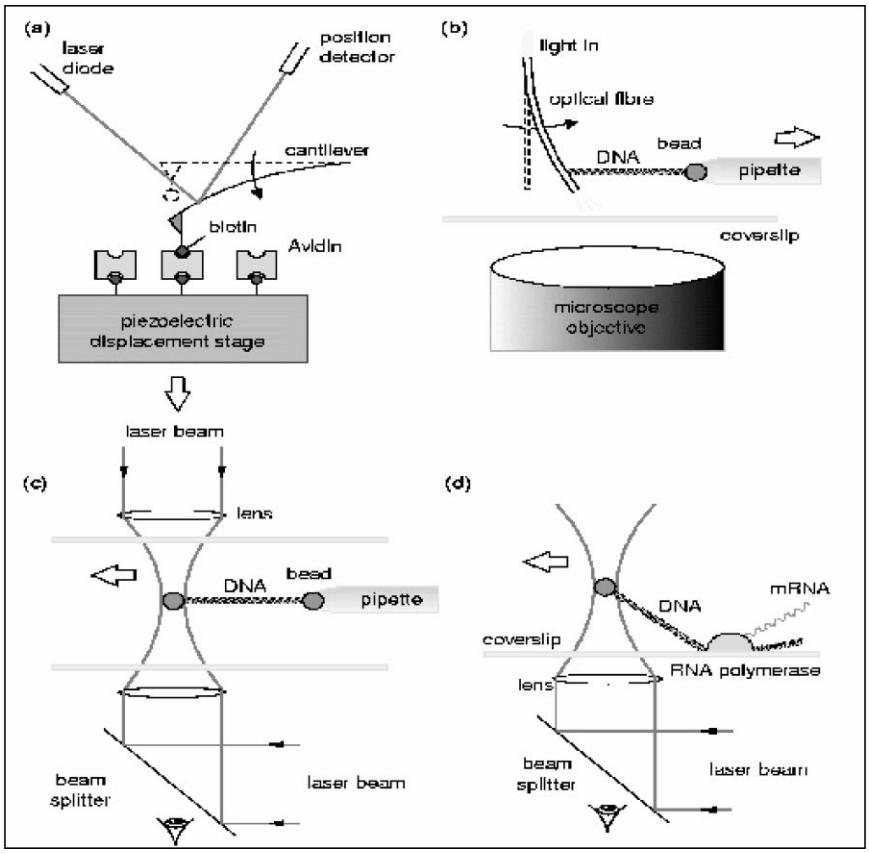

Fig. 1. Example of forces transducers used in various experiments. (a) An AFM cantilever is often used as a force transducer during intermolecular force measurements (Florin et al., 1994) and protein unfolding experiments (Rief et al., 1997). Its deflection upon pulling is detected by the displacement of a laser beam reflected from the cantilever. (b) In some of the experiments involving DNA pulling (Cluzel et al., 1996; Léger et al., 1998) and unzipping (Essevaz-Roulet et al., 1997), the force transducer is an optical fiber, which deflection is detected optically (by measuring the displacement either of the fiber directly on a microscope stage or of a light beam emitted from its pulled end). (c) In the experiment of Bustamante and coworkers (Smith et al., 1996; Kellermayer et al., 1997), the force transducer is an optical trap consisting of two co-axial counter-propagating and focused laser beams. The displacement of the bead in the trap is observed with a microscope and together with the trap stiffness is used to assess the trapping force. (d) A force transducer often used to characterize molecular motors (Simmons et al., 1996; Finer et al., 1994; Yin et al., 1995) is the optical tweezers which consists of a single strongly focused laser beam holding a bead in its focal point. Force measurement is carried out as in (c). Figure, courtesy of *Structure* (Bensimon, 1996).

immunological assays (immuno-PCR) (Sano et al., 1992). Most of these applications achieve the required binding specificity via biochemical reactions between a (possibly modified) DNA molecule and an appropriately treated surface. For example, the extremity of the molecule can be functionalized with biotine (or digoxigenine) which can interact specifically with streptavidine (or an antibody to digoxigenine) bound to a surface (Smith et al., 1992). Similarly, surfaces coated with oligonucleotides can be used to recognize the complementary extremity of DNA molecules.

Finally, there exist a large range of chemical methods to anchor (with various degrees of specificity) the extremities of DNA to surfaces bearing reactive groups (e.g. primary or secondary amine, carboxyl or thiol moieties).

An interesting alternative which does not require any modification of the molecule relies on the specific adsorption of DNA by its ends on hydrophobic surfaces at a pH $\sim$5.5 (Allemand et al., 1997). On many different hydrophobic materials (teflon, polystyrene, graphite, silanised glass, etc.) DNA was observed to adhere strongly and non-specifically at low pH and weakly or not at all at high pH. In between there exists a narrow pH range (pH $= 5.5 \pm 0.2$) where DNA binds to the surface by its extremities only.

Once DNA is anchored to a surface by its end(s), a very easy way to stretch it is to drain the solution (e.g. by pulling the surface out of it or by letting it evaporate), see Fig. 2. In that process, known as molecular combing, the anchored DNA molecules are aligned on the surface by the receding meniscus as are algae on the shore by the receding tide. It has been shown that the force applied on the molecule by the receding air/water interface (estimated to be $\sim$160 pN) is large enough to stretch it but not to break its bond(s) with the surface (Bensimon et al., 1994, 1995). Because this force is acting locally (at the interface), DNA is stretched uniformly (Allemand et al., 1997): $\sim$1 μm for every 2 kbytes. Fluorescent in situ hybridization (FISH) on combed molecules (Bacs, Yacs or even whole genomes) allows one to obtain very accurate ($\sim$1 kbps) genomic maps (Weier et al., 1995; Michalet et al., 1997). The ordering, orientation and distance between genes, the existence of genomic rearrangements (e.g. deletions) can thus be determined.

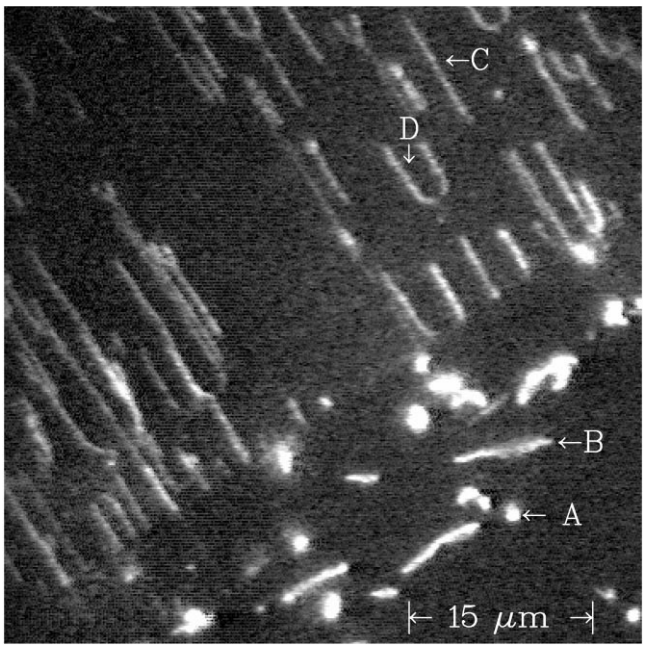

Fig. 2. Molecular combing of λ−DNA stained with YOYO1. The molecules in solution (bottom) are bound at one (A) or both (B) ends. The meniscus extends across the image from the lower left to upper right. The extended molecules left behind the meniscus are visible as straight segments (C) if bound at one end, or loops (D) if bound at both ends.

Observation of the combing of DNA molecules grafted at both ends to a surface is instructive, see Fig. 3. First as the meniscus moves past the anchoring points of the molecule it stretches its two anchored segments (legs) *perpendicular* to the interface. The portion of the molecule in solution decreases until it spans the distance between the two legs. It is then stretched *parallel* to the contact line, its length diminishing as the meniscus recedes thus forming a loop. Then as the tension in the molecule increases the loop breaks. The length of the DNA molecule at the breaking point l_b can be measured and compared with the unstretched length $l_{b,0}$, see Fig. 3. It turns out that $l_b/l_{b,0} = 2.14 \pm 0.2$ (Bensimon et al., 1995): DNA can be extended to more than twice its length before breaking! As we shall see below, this huge deformation of DNA (it is similar to the ratio of the interphosphate distance to the distance between base-pairs) has to be accommodated by a profound restructuring of the Watson–Crick double helix.

2.2. DNA manipulation and force measurements

Once DNA has been bound to a surface, it can be manipulated by displacing the anchoring object. The first manipulations of DNA molecules involved translating with the help of optical tweezers a small streptavidine-coated bead to which a single biotynilated DNA had been anchored (Chu, 1991; Perkins et al., 1994a,b). The molecule stained with a fluorescent dye was stretched by the hydrodynamic drag and its relaxation in various conditions was studied. In particular when stretched in a dilute solution of other DNA molecules the relaxation of the molecule provided the first direct observation of the reptation dynamics of an entangled polymer.

By anchoring a DNA at both ends to different surfaces (typically a coverslip, a microbead or a microneedle), a force can be exerted on the molecule by displacing the surfaces relative to each other. Thus, DNA can be anchored to an AFM cantilever (or microfiber) at one end and to a

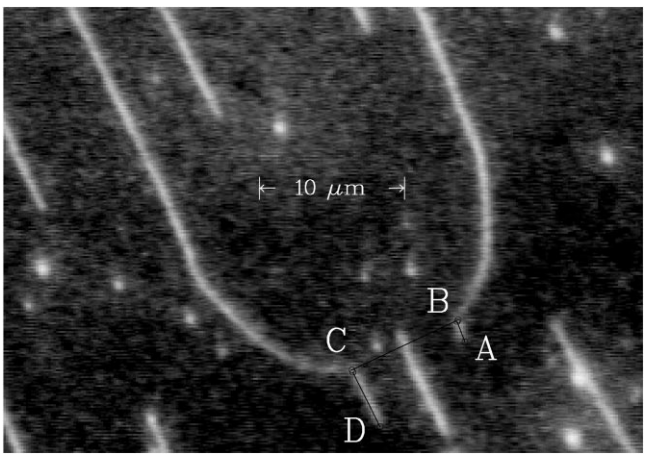

Fig. 3. Fragment of the genomic DNA, of one of the authors combed on a hydrophobic surface. The DNA bound at both ends form a typical broken loop. From measurements on such figures we deduce the extension of DNA at the breaking point: the stretched molecule length is $l_b = \overline{BC}$, its unstretched length $l_{b,0}$ is deduced by dividing the length $\overline{AB} + \overline{DC}$ by the extension factor observed for a straight molecule combed on an hydrophobic surface (1 μm for 2 kbytes).

treated surface at the other (Engel et al., 1999; Rief et al., 1999, 1997; Florin et al., 1994). By displacing the surface, see Fig. 1, the molecule is stretched and pulls on the cantilever. Knowing its spring constant, the force on the molecule can be measured. Very high forces (many thousands of pN) can be achieved and measured in these experiments with a precision of $\sim$10 pN and a spatial resolution of $O(0.1\ \text{nm})$.

By using two co-axial counter-propagating laser beams a small transparent bead can be trapped, see Fig. 1 with a force of $O(100\ \text{pN})$ and a spatial resolution $\sim$10 nm. The force exerted on the bead can be deduced from the displacement of the trapping beam due to its refraction in the bead, i.e. by directly measuring the momentum transfer (Smith, 1998). This absolute measure bypasses the need for a calibration of this optical trap.

Another popular technique involves the stretching by an intensely focused laser beam (optical tweezers (Simmons et al., 1996)) of a transparent bead of radius r of $O(1\ \mu\text{m})$ anchored by a DNA molecule to a surface, see Fig. 1. Forces $F < 50$ pN can be achieved and measured with a precision of $\sim$0.1 pN by following the displacement δx of the trapped bead from its equilibrium (zero force) position: $F = k_{\text{trap}}\delta x$, where k_{trap} is the elastic stiffness of the optical trap. δx can be measured with a precision of $O(1\ \text{nm})$ (Simmons et al., 1996), enough to resolve a single step of myosin (Finer et al., 1994; Saito et al., 1994) or kinesin (Schnitzer and Block, 1997; Hua et al., 1997). k_{trap} has to be determined prior to any force measurement, for example by pulling on the bead with a known force such as the hydrodynamic drag F_s of a fluid (of viscosity η) flowing with velocity v around the bead: $F_s = 6\pi\eta r v$. Alternatively, one may determine k_{trap} by measuring the intensity of the Brownian fluctuations $\langle \delta x^2 \rangle$ of the trapped bead. By the equipartition theorem they have to satisfy (Simmons et al., 1996; Einstein, 1956; Reif, 1965):

$$\frac{k_{\text{trap}}\langle \delta x^2 \rangle}{2} = \frac{k_B T}{2}. \tag{1}$$

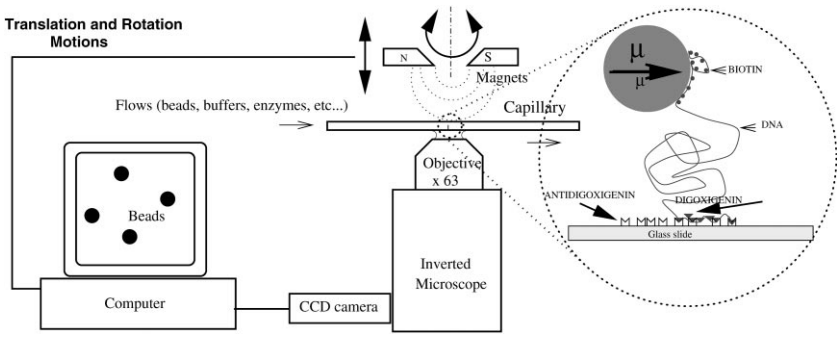

Fig. 4. Schematic view of the apparatus used to twist and stretch single DNA molecules. DNA molecules were first prepared with *biotin* attached to one end and *digoxigenin* (*dig*) bound to the other. These end-labeled DNA molecules are incubated with *streptavidin*-coated magnetic beads and then flowed into a square glass capillary coated with an antibody to *dig, antidig*. The DNA molecules bind specifically to the bead via *biotin/streptavidin* coupling and to the glass via *dig/antidig* coupling. The capillary is placed above an inverted microscope. Magnets are placed above the capillary. By approaching the magnets we increase the stretching force on the bead and thus on the molecule. By rotating the magnets the molecule is twisted at constant force. A frame grabber installed in a PC allows for tracking of the Brownian fluctuations $\langle \delta x^2 \rangle$ of the bead. The determination of $\langle \delta x^2 \rangle$ and of the molecule's extension l leads to a measure of the stretching force $F = k_B T l / \langle \delta x^2 \rangle$.

To twist and stretch a DNA molecule and study its interactions with proteins, a magnetic trapping technique (Strick et al., 1996) has proved particularly convenient. Briefly, it consists in stretching a single DNA molecule bound at one end to a surface and at the other to a magnetic micro-bead (1–4.5 μm in diameter), see Fig. 4. Small magnets, whose position and rotation can be controlled, are used to pull on and rotate the micro-bead and thus stretch and twist the molecule. This system allows one to apply and measure forces ranging from a few fN (10^{-3}pN) to nearly 100 pN (see Strick et al., 1998b) with a relative accuracy of $\sim 10\%$.

In contrast with other techniques, this force measurement is absolute and does not require a calibration of the sensor. It is based on the analysis of the Brownian fluctuations of the tethered bead, which is completely equivalent to a damped pendulum of length $l = \langle z \rangle$ pulled by a magnetic force F (along the z-axis). Its longitudinal ($\delta z^2 = \langle z^2 \rangle - \langle z \rangle^2$) and transverse δx^2 fluctuations are characterized by effective rigidities $k_{||} = \partial_z F$ and $k_\perp = F/l$. By the equipartition theorem they satisfy (Einstein, 1956; Reif, 1965)

$$\delta z^2 = \frac{k_B T}{k_{||}} = \frac{k_B T}{\partial_z F}, \tag{2}$$

$$\delta x^2 = \frac{k_B T}{k_\perp} = \frac{k_B T l}{F}. \tag{3}$$

Thus from the bead's Brownian fluctuations ($\delta x^2, \delta y^2$) one can extract the force pulling on the molecule (the smaller the fluctuations the greater F) and from δz^2 one obtains its first derivative, $\partial_z F$. This measurement method can be used with magnetic (but not optical) traps because the variation of the trapping gradients occurs on a scale ($O(1\,\text{mm})$) much larger than the scale on which the elasticity of the molecule changes ($O(0.1\,\mu\text{m})$). In other words, the stiffness of the optical trap is very large compared to F/l. A further bonus of the magnetic trap technique is that measurements on DNA at constant force are trivial (just keep the position of the magnets fixed). With cantilevers or optical tweezers to work at constant force requires an appropriate feedback to ensure that the displacement of the sensor is kept constant. However, because its stiffness depends on the force, the magnetic trap technique has at weak forces (< 1 pN) a lower spatial resolution of $O(10\,\text{nm})$, than the other manipulation methods. Finally notice that by using electro-magnets, a faster and more versatile magnetic tweezers system has recently been developed (Gosse and Croquette, 1999).

3. Models of polymer elasticity

Just like any polymer in solution, free DNA adopts a random coil conformation which maximizes its entropy (de Gennes, 1979). Pulling on the molecule reduces this entropy and costs energy. The associated entropic forces result from a reduction of the number of possible configurations of the system consisting of the molecule (be it a polymer, DNA or a protein) and its solvent (water, ions), so that at full extension there is but one configuration left: a straight polymer linking both ends. To reach that configuration work has to be done against entropy, a force has to be applied. The entropic forces are rather weak, typically < 10 pN. Beyond this regime and up to about 70 pN DNA stretches like any spring: it is in an enthalpy dominated regime.

3.1. The Kratky–Porod model

For simplicity, let us first consider a polymer chain with no torsional stress. Such a chain is often described by the Kratky–Porod model (Cantor and Schimmel, 1980): a succession of N segments of length b and orientation vector $\mathbf{t}_i$, see Fig. 5. The energy $\mathscr{E}_{\mathrm{KP}}$ of a given chain configuration (the ensemble of segment orientations $\{\mathbf{t}_i\}$) is the sum of the bending energies of successive segments:

$$\mathscr{E}_{\mathrm{KP}} = -\frac{B}{b}\sum_{i=2}^{N} \mathbf{t}_i \cdot \mathbf{t}_{i-1} = -\frac{B}{b}\sum_{i=2}^{N} \cos\theta_i, \tag{4}$$

where θ_i is the angle between successive orientation vectors and B is the bending modulus. (Notice the analogy between the statistical mechanics of a Kratky–Porod chain and that of a classical one-dimensional magnetic (spin) system (Fisher, 1964).) This model has been solved exactly (Fisher, 1964). The angular correlation decays exponentially with distance along the chain:

$$\langle \mathbf{t}_i \cdot \mathbf{t}_j \rangle = \mathrm{e}^{-b|i-j|/\xi_T}, \tag{5}$$

where $\xi_T = B/k_{\mathrm{B}}T$ is the decay length of the angular correlation. It reflects the stiffness of the chain and is known as the persistence length. The chain end-to-end mean square distance R_g satisfies

$$R_g^2 \equiv \langle \mathbf{R}^2 \rangle = \left(b\sum_{i=1}^{N} \mathbf{t}_i \right)^2 \simeq 2Nb\xi_T = 2l_0\xi_T, \tag{6}$$

where $l_0 = Nb$ is the chain length. A DNA molecule in solution thus adopts a fluctuating random coil configuration of typical size R_g, known as the gyration radius. For many years, the measurement of R_g by various means (sedimentation, light scattering, etc. (Cantor and Schimmel, 1980; Hagerman, 1988) was the only way to estimate the persistence length of DNA (or any polymer).

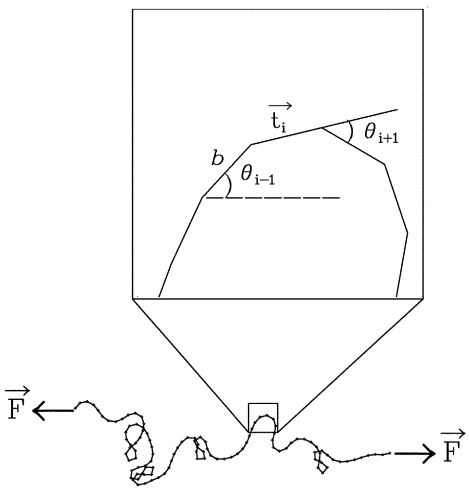

Fig. 5. A continuous polymer chain can be simulated by a chain of freely rotating segments of size b and orientation vector $\mathbf{t}_i$. The direction of the stretching force F defines the z-axis.

The stretching of a single DNA molecule now provides a much more precise way of measuring ξ_T. To model the behavior of a polymer chain under tension, it suffices to add to Eq. (4) a term representing the work $W = -\mathbf{F}\cdot\mathbf{R} = -Fb\sum t_{i,z} = -Fb\sum\cos\Theta_i$ done by a force F acting on the chain along the $z-$axis (Θ_i is the angle between $\mathbf{t}_i$ and the $z-$axis):

$$\mathscr{E}_{\mathrm{KP}} = -\frac{B}{b}\sum_{i=2}^{N}\mathbf{t}_i\cdot\mathbf{t}_{i-1} - Fb\sum_{i=1}^{N}t_{i,z} = -\frac{B}{b}\sum_{i=2}^{N}\cos\theta_i - Fb\sum_{i=1}^{N}\cos\Theta_i. \tag{7}$$

Unfortunately, this model can be solved only for small forces, where the mean extension of the chain $l \ll l_0$ (Fisher, 1964) is

$$l = \frac{2F\xi_T}{3k_{\mathrm{B}}T}\,l_0 = \frac{F}{3k_{\mathrm{B}}T}\,R_g^2. \tag{8}$$

To compute the elastic response of a chain at higher forces one has to resort to numerical calculations (e.g. transfer matrix methods) or to various approximations of the Kratky–Porod model.

3.2. The freely jointed chain model

An interesting limit is the freely jointed chain (FJC) model, which consists in setting $B = 0$ in Eq. (7). It models a chain whose segments are unrestricted in their respective orientation and corresponds to a discretization of a polymer with segments of length $b = 2\xi_T$ (the so-called Kuhn length). In the FJC model the energy of a given chain configuration $\{\mathbf{t}_i\}$ is thus $\mathscr{E}_{\mathrm{FJC}} = W = -Fb\sum\cos\Theta_i$. The partition function $\mathscr{Z}$ is

$$\mathscr{Z} = \sum_{\mathbf{t}_i}\mathrm{e}^{-\mathscr{E}_{\mathrm{FJC}}/k_{\mathrm{B}}T} = \sum_{\mathbf{t}_i}\prod_{i=1}^{N}\mathrm{e}^{Fb\cos\Theta_i/k_{\mathrm{B}}T} \tag{9}$$

$$= \left[\int \mathrm{d}\Omega\,\mathrm{e}^{Fb\cos\Theta/k_{\mathrm{B}}T}\right]^N = \left[\frac{2\pi k_{\mathrm{B}}T}{Fb}\sinh\frac{Fb}{k_{\mathrm{B}}T}\right]^N. \tag{10}$$

From the free energy $\mathscr{F} = -k_{\mathrm{B}}T\log\mathscr{Z}$, one can compute the mean extension of the chain l

$$l = -\frac{\partial\mathscr{F}}{\partial F} = l_0\left(\coth\frac{Fb}{k_{\mathrm{B}}T} - \frac{k_{\mathrm{B}}T}{Fb}\right). \tag{11}$$

Notice that at small forces one recovers our previous result, Eq. (8). However, as shown in Fig. 6, the FJC model is too crude and is *not* a good approximation of the elastic behavior of a DNA molecule at large extensions ($l > R_g$).

3.3. The worm like chain model

A much more precise description is afforded by the worm like chain (WLC) model, the continuous ($b \to 0$) limit of Eq. (7):

$$\frac{\mathscr{E}_{\mathrm{WLC}}}{k_{\mathrm{B}}T} = \frac{\xi_T}{2}\int_0^{l_0}\left(\frac{\mathrm{d}\mathbf{t}}{\mathrm{d}s}\right)^2\mathrm{d}s - \frac{F}{k_{\mathrm{B}}T}\int_0^{l_0}\cos\Theta(s)\,\mathrm{d}s, \tag{12}$$

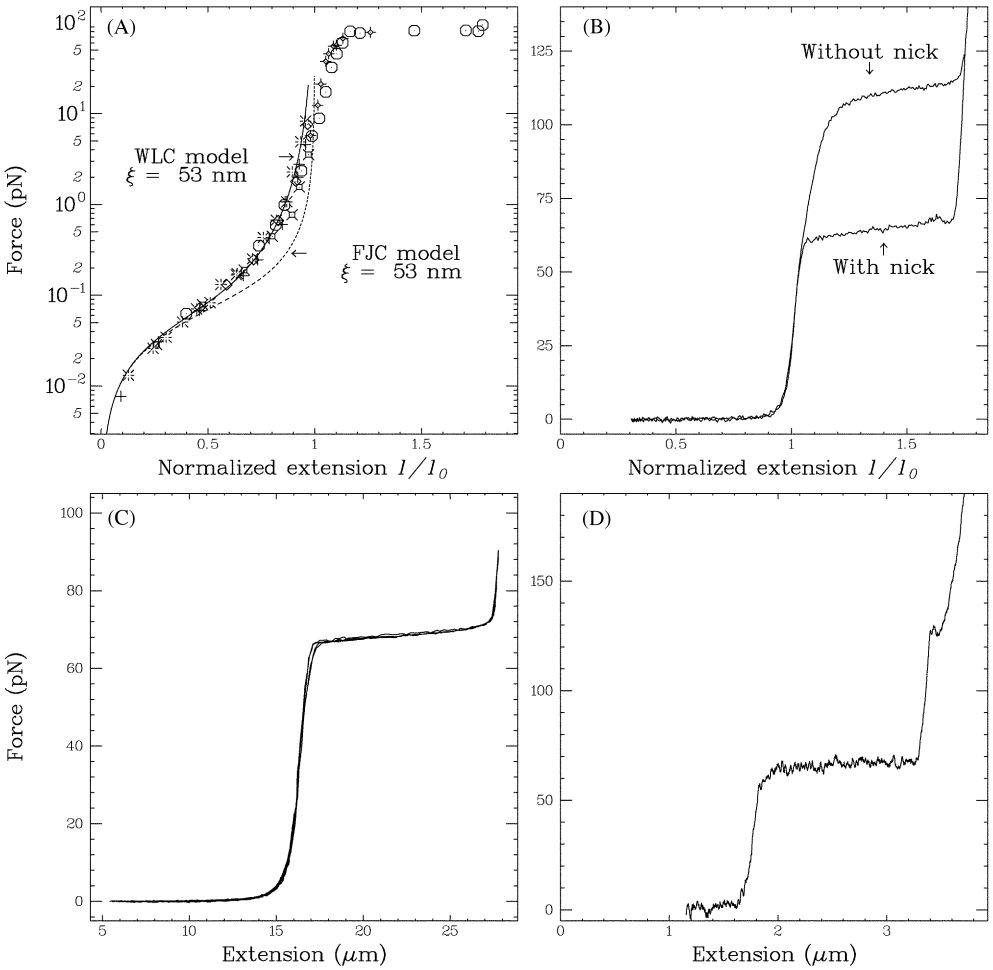

Fig. 6. Force versus extension curves of single DNA molecules obtained by different groups. (A) The dots correspond to several experiments performed over a wide range of forces. The force was measured using the Brownian fluctuation technique (Strick et al., 1996). The full line curve is a best fit to the WLC model for forces smaller than 5 pN. The dashed curve is the result of the FJC model with the same persistence length (it is clearly a worse description of the behavior of DNA under stress than the WLC model). At high forces, the molecule first elongates slightly, as would any material in its elastic regime. Above 70 pN, the length abruptly increases, corresponding to the appearance of a new structure called S-DNA. (B) The same transition observed by J.-F. Léger and D. Chatenay using a glass needle deflection on a nicked molecule and an unnicked molecule (the transition occurs for a higher force). (C) The transition is also observed by S. Smith and C. Bustamante using optical tweezers. (D) Finally, H. Clausen-Schaumann and H. Gaub observe also the transition using an AFM. (We thank C. Bustamante, D. Chatenay, H. Clausen-Schaumann, H. Gaub, J.-F. Léger and S. Smith for sharing their data).

where s is the curvilinear coordinate along the chain. The calculation of the partition function $\mathscr{Z}$ and the free energy $\mathscr{F}$ of that model calls upon an analogy with the quantum mechanical problem of a dipole in an electric field, which is beyond the scope of this paper. It has however been solved by Marko and Siggia (Fixman and Kovac, 1973; Bustamante et al., 1994; Vologodskii, 1994; Marko and Siggia, 1995a,b). Though there is no analytic formula equivalent to Eq. (11) for the

force vs. extension behavior of a WLC, a simple and efficient numerical solution was recently provided by Bouchiat et al. (1999), who gave an approximation better than 0.1%:

$$F = (k_B T/\xi_T) g(x), \tag{13}$$

where $x = l/l_0$ and

$$g(x) = x - \frac{1}{4} + \frac{1}{4(1-x)^2} + \sum_{i=2}^{7} a_i x^i \tag{14}$$

with $a_2 = -0.5164228$, $a_3 = -2.737418$, $a_4 = 16.07497$, $a_5 = -38.87607$, $a_6 = 39.49944$, $a_7 = -14.17718$ (Bouchiat et al., 1999). Notice that at small relative extensions $x \ll 1$, as for the FJC model we recover Eq. (8). However, when compared over the whole extension range, the WLC model is a much better description of the behavior of DNA than the FJC model. As shown in Fig. 6 the WLC model fits extremely well the measured data and allows a very precise estimation of the DNA's persistence length: $\xi_T = 52 \pm 2$ nm in physiological conditions (10 mM phosphate buffer (pH = 7.5), 10 mM NaCl).

3.4. Self-avoidance effects

In the theoretical models described previously, the fact that a real polymer cannot intersect itself was not taken into consideration. For example in the computation of the partition function $\mathcal{Z}$, Eq. (10), we included these unrealistic configurations. In that section we shall try to justify this approach. A treatment of the self-avoidance effects of a stretched polymer exists only at low extensions ($l \ll l_0$), where a heuristic argument due to Flory (1975) works remarkably well. Due to self-avoidance one expects a real chain to occupy a larger volume than the so-called Gaussian (intersecting or phantom) chains considered previously, which occupied a volume R_g^3. That of course cost some entropic energy which is, however, compensated by a reduction in the probability of interaction. In this approach the free energy of a FJC polymer is (recall that at low extensions all models are equivalent):

$$\frac{\mathcal{F}}{k_B T} = \frac{3l^2}{2R_g^2} + \frac{vN^2}{l^3}. \tag{15}$$

The first term on the right describes the energy cost associated with a swelling of the polymer ($\sim \int F \, dl$, with F given by Eq. (8)). The second term accounts for the self-avoidance. It is proportional to the probability that two segments of the FJC of volume $v = \pi r^2 b$ will share the same location in the space l^3 occupied by the chain (the segments are assumed cylindrical with a radius r and length b). That repulsive term decreases as the chain swells. By minimizing $\mathcal{F}$ with respect to l, one obtains the equilibrium (Flory's) radius of a self-avoiding polymer:

$$R_F = (vb^2)^{1/5} N^{3/5}. \tag{16}$$

Excluded volume interactions will become important when in the volume explored by one monomer, typically b^3 there is another monomer, i.e. when the monomer concentration $c = N/R_F^3 = 1/b^3$. Self-avoidance thus becomes non-negligible when $N > (b/r)^{3/2}/\pi^{3/4}$. For a DNA molecule with $r = 1$ nm and $b = 100$ nm, this corresponds to $N \sim 400$, i.e. a molecular length: $l_{0,F} = Nb \sim 40\,\mu$m. Almost all manipulations of DNA molecules so far have been in a

regime $l_0 < l_{0,F}$, where self-avoidance is totally negligible. That is except in torsionally constrained experiments where self-avoidance is crucial as it stabilizes plectonemic loops (see Section 4 below).

3.5. Beyond the entropic regime

Beyond the entropic regime, i.e. from $\sim$6 pN to about 70 pN, DNA behaves like an elastic rod with stretch modulus $EA \sim 1000$ pN (Smith et al., 1996; Wang et al., 1997) (where E is the Young modulus of DNA and A its effective cross-sectional area (Hogan and Austin, 1987)). Neglecting entropic contributions, the force vs. extension curve follows a simple Hookean law (as any elastic material): $F = EA(x - 1)$ (with $x = l/l_0 > 1$). Some ad hoc formulas exist, interpolating between the entropic and Hookean regimes, e.g. replacing the term $(1 - x)^2$ in Eq. (14) by $(1 - x + F/EA)^2$ (Wang et al., 1997).

Finally at about 70 pN a surprising transition has recently been discovered where DNA stretches to about 1.7 times its crystallographic length (Smith et al., 1996; Cluzel et al., 1996). As characteristic of the first-order transitions in nature (e.g. boiling) that transition is highly cooperative: a small change in force results in a large change in extension (see Fig. 6). A phenomenological description of that transition has been proposed (Cluzel et al., 1996; Cizeau and Viovy, 1997; Ahsan et al., 1998; Marko, 1998), where the force plays the same role as the magnetic field in a ferromagnetic context. In this model, the observed sharpness of the transition (its high cooperativity) is associated with a large interfacial energy between the phases, suggesting that the typical domain size is about 100 bases long (Cizeau and Viovy, 1997).

To address the possible structural modification in the molecule resulting from pulling on it, a numerical energy minimization of DNA under stress was performed by R. Lavery and collaborators (Cluzel et al., 1996; Lebrun and Lavery, 1996). Its results reveal the existence of a new conformation called S-DNA indeed 70% longer than B-DNA, whose exact structure depends on which extremities of the DNA are being pulled (3′–3′ or 5′–5′). If both 3′ extremities are being pulled the double helix unwinds upon stretching. The final structure resembles a ladder. If both 5′ ends are pulled a helical structure is preserved. It is characterised by a strong base pair inclination, a narrow minor groove and a diameter roughly 30% less than that of B-DNA. In both cases the rupture of the molecule (by unpairing of the bases) occurs as observed during molecular combing (Bensimon et al., 1994, 1995) when its extension is more than twice that of B-DNA (Wilkins et al., 1951).

These numerical results are supported by experiments done almost 50 years ago by Wilkins et al. (1951) before the double helix structure of DNA was even proposed. Those suggested that stretched DNA fibers indeed undergo a transition to a structure with tilted bases about twice longer than the relaxed molecule. However, recent experiments by Léger et al. (1999) stretching torsionally constrained single molecules have shown that the S-DNA phase has a helical pitch of 22 nm with 38 bases per right-handed turn, which would make it look more like a slightly twisted ladder.

The existence of a new stable form of DNA at high extension might have considerable interest for the study of DNA/protein interactions. Thus RecA is known to induce a 60% extension of B-DNA (Stasiak and Di Capua, 1982; Stasiak et al., 1983) and facilitate the formation of a triple helix, a putative intermediate during recombination. Smith et al. (1996) calculated that the

existence of an extended S-form of DNA reduced the energetics of RecA binding to DNA by as much as $15k_BT$ (9 kcal/mol) per complex. Recent experiments (Léger et al., 1998; Shivashankar et al., 1999; Hegner et al., 1999) have indeed shown that the polymerisation of RecA on a dsDNA was facilitated by stretching the molecule. This implies that the barriers to nucleation and accretion of a RecA fiber on DNA is lowered by the presence of a S-DNA sub-phase. Numerical modeling further suggest that its structure is closer to the RecA/DNA complex than regular B-DNA (Lebrun and Lavery, 1997).

3.6. Elasticity of heterogeneous polymers

In the preceding discussion, the polymer properties were assumed homogenous, i.e. we did not consider possible sequence specific effects on the elastic behavior of DNA. The Kratky–Porod model allows one to treat those to some extent. It is thus easy to introduce some local preferred bending (i.e. orientational angle ψ_i between successive segments) by replacing the term $\cos\theta_i$ in Eq. (7) by $\cos(\theta_i - \psi_i)$. The case where the ψ_i's are fixed randomly along the chain, thus defining a static (disorder induced) angular correlation ξ_d, has been analysed by two groups using slightly different models (Bensimon et al., 1998; Nelson, 1998). Surprisingly, it turns out that the elastic behavior of such a heterogeneous chain is to all practical purposes identical to that of an homogenous WLC with an effective persistence length ξ_{eff} which is a model-dependent function of ξ_d and ξ_T. Therefore, one does not expect sequence specific effects to alter drastically the results of the WLC model described previously. It is worth emphasizing the theoretical point that sequence inhomogeneities must be treated as 'quenched', i.e. the free energy of the system should be averaged over the disorder (Binder and Young, 1986). Some results claiming to describe sequence disorder effects (Nelson, 1998; Trifonov et al., 1987; Schellman and Harvey, 1995) actually employ an 'annealed' averaging of the partition function over disorder which is mathematically simpler but is irrelevant to experiment where the sequence is fixed.

4. DNA under torsion

4.1. Topological properties of coiled DNA

To describe DNA under torsional stress it is first necessary to introduce some topological concepts. The first is the twist (Tw), the number of helical turns along the molecule. For a torsionally unconstrained B-DNA, $\mathrm{Tw} = \mathrm{Tw}_0 = N/h$ where N is the number of base-pairs and $h = 10.4$ is the number of base-pairs per turn of the helix. The second topological quantity of interest is the writhe (Wr) of the molecule. Wr is a measure of the coiling of the DNA axis about itself, as a twisted phone cord which forms interwound structures in order to relieve its torque. If the DNA molecule is torsionally constrained, then the total number of times the two strands of the helix cross each other (either by twist or writhe) is a topological invariant of the system called the linking number $\mathrm{Lk} = \mathrm{Tw} + \mathrm{Wr}$ (White, 1969). For relaxed linear DNA molecules, assuming the absence of any spontaneous local curvature, $\mathrm{Lk} = \mathrm{Lk}_0 = \mathrm{Tw}_0$. The relative difference in linking number between the supercoiled and relaxed forms of DNA is called the degree of

supercoiling, σ:

$$\sigma = (\mathrm{Lk} - \mathrm{Lk}_0)/\mathrm{Lk}_0 = \Delta\mathrm{Lk}/\mathrm{Lk}_0. \tag{17}$$

The value of σ for most circular molecules isolated from cells or virions is roughly -0.06. A notable exception occurs in hyperthermophilic archeabacteria (Woese and Fox, 1977; Woese et al., 1990) who have a positively coiled DNA (Kikuchi and Asai, 1984; Forterre, 1996). In the experiments described here, provided that the anchoring of the DNA molecule is achieved at multiple points at both ends, a torsional constraint can be applied on the molecule by simply rotating the magnets. As one turn of the magnets implies a change of one turn of the molecule, we have simply $\Delta\mathrm{Lk} = \pm n$, where $\pm n$ is the number of turns by which the magnets are made to rotate. Note that at fixed Lk the ratio Tw/Wr will depend on the force stretching the molecule, the writhe being suppressed by high forces. As a consequence, pulling on a coiled molecule increases the torque twisting it, until its writhe reaches zero.

4.2. The mechanical buckling instability

Twisting DNA leads to a torsional buckling instability analogous to that observed on telephone cords or rubber tubes. This instability leads to the formation of interwound structures known as supercoils or plectonemes. Of course, a DNA molecule is also animated by very strong thermal fluctuations which play an important role. However, it is instructive to first consider the purely mechanical (zero-temperature) instability of a rubber tube of length l and torsional modulus C. If we firmly hold one end of the tube while simultaneously rotating and pulling on the second end with a force F, we observe the following phenomenon (see Fig. 7): when the twist constraint is small, the associated torque Γ increases linearly with the twist angle θ, $\Gamma = C\theta/l$ and the tube remains straight. As the tube is further twisted, a critical twist angle $\theta_{\mathrm{c,b}}$ and torque $\Gamma_{\mathrm{c,b}}$ are reached where the tube ceases to be straight: it locally buckles and forms a small loop of radius $R_{\mathrm{c,b}}$. The torsional energy thus gained is $2\pi\Gamma_{\mathrm{c,b}}$, whereas the energy cost (due to bending and work against F) is (see Eq. (12)): $\mathscr{E} = \pi B/R + 2\pi RF$. The cost is minimized for a loop of radius $R_{\mathrm{c,b}} = \sqrt{B/2F}$. The critical torque for the formation of plectonemes is controlled by the balance between energy gain and cost, i.e. by the stretching force:

$$\Gamma_{\mathrm{c,b}} = \mathscr{E}_{\min}/2\pi = \sqrt{2BF}. \tag{18}$$

As we twist the tube further, we increase the length of the plectonemes but the torque in the tube remains basically fixed at its critical value $\Gamma_{\mathrm{c,b}}$.

4.3. DNA under torsion: the rod like chain model

For DNA, the picture is pretty much the same (Bouchiat and Mézard, 1998; Moroz and Nelson, 1998; Vologodskii and Marko, 1997). The thermal fluctuations which will be most important near the mechanical instability at $\theta_{\mathrm{c,b}}$ will tend to round it off. Hence as one is coiling a DNA molecule under fixed force F, one observes the following behavior (see Fig. 7): at low degrees of supercoiling $|\sigma|$ the molecule's extension varies little. Beyond a critical value σ_{c} (which depends on the force), the molecule shortens continuously as it is twisted further. A theoretical treatment of this behavior is given by the RLC model developed by Bouchiat and Mézard (1998,

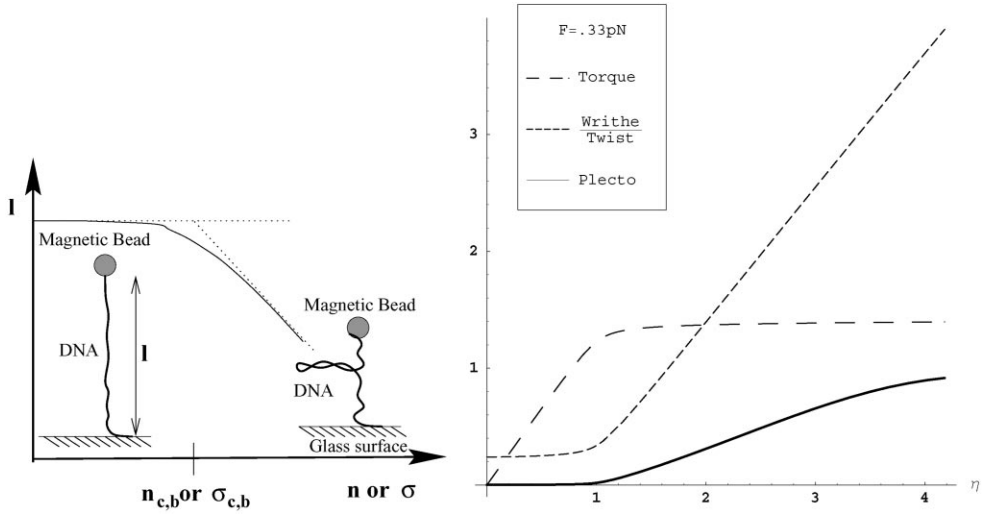

Fig. 7. LEFT: schematic view of the buckling transition for a twisted rubber tube (dotted line) or a DNA molecule (solid line). Below a critical number of turns $n_{c,b}$ the rubber tube's torque increases linearly as it stores twisting energy. When $n_{c,b}$ turns have been added the system abruptly exchanges twisting energy for bending energy and plectonemes begin to form. The plectonemes grow linearly with subsequent twisting and the torque remains constant thereafter. In the case of DNA the same picture holds, except for the fact that thermal fluctuation round off the transition which takes place at $n_{c,b}$. RIGHT: Results from the RLC model corresponding to a stretching force of $F = 0.33$ pN. The x-axis represents the supercoiling variable $\eta = 2\pi n \xi_T / l_0 \simeq 95\sigma$ (Bouchiat and Mézard, 1998), and the y-axis is in arbitrary units. The long-dash curve represents the torque acting on the DNA: as decribed above, it increases linearly until $\eta_{c,b} \sim 1$ ($\sigma \sim 0.01$) and remains essentially constant thereafter. The short-dash curve represents the ratio of writhe to twist: note that the writhe is never zero and increases rapidly as $\eta > 1$. Finally, the full line measures the fraction of plectonemes in DNA: stable supercoiled structures only appear after the torsional buckling transition has been passed.

1999) which consists in describing a DNA molecule not as a chain free to rotate but as a rod with a finite torsional modulus C. The energy of this rod like chain (RLC) model $\mathscr{E}_{\mathrm{RLC}}$ is obtained by adding to the energy of the WLC model, Eq. (12), an energy of twist $\mathscr{E}_{\mathrm{T}}$:

$$\mathscr{E}_{\mathrm{RLC}} = \mathscr{E}_{\mathrm{WLC}} + \mathscr{E}_{\mathrm{T}} = \mathscr{E}_{\mathrm{WLC}} + \frac{C}{2}\int_0^{l_0} \mathrm{d}s\, \Omega^2(s), \tag{19}$$

where $\Omega(s)$ is the local twist of the chain. A detailed solution of this model which is beyond the scope of the present paper can be found in Bouchiat and Mézard (1998, 1999) and Moroz and Nelson (1998a,b). A particular mathematical subtely of this model is that the twist integrant in Eq. (19) is singular. That singularity has to be regularized either by a truncation of its series expansion (Moroz and Nelson, 1998a,b) or by the reintroduction of the short length cut-off b of the Kratky–Porod model (Bouchiat and Mézard, 1998; Bouchiat et al., 1999). Although the RLC model neglects the chain's self-avoidance, which stabilizes the plectonemes, its predictions fit remarkably well with our observations at low forces (<0.4 pN) where as the molecule is coiled its end to end distance decreases, see Fig. 8. From a fit of the RLC predictions to our data, one can extract a value for the torsional modulus C of DNA: $C/k_{\mathrm{B}}T = 86 \pm 5$ nm (Bouchiat and Mézard,

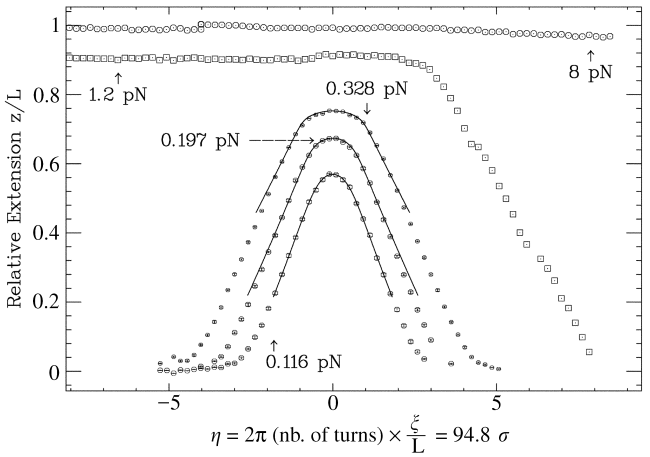

Fig. 8. Relative extension of a DNA molecule vs. the degree of supercoiling $\eta = 2\pi n\xi_T/l_0 \simeq 95\sigma$ for various stretching forces. For the three curves obtained at low force, the behavior is symmetrical under $\sigma \to -\sigma$. The shortening corresponds to the formation of plectonemes upon writhing. For these low forces the comparison between the experimental data (points) and the rod like chain model with $C/k_BT = 86$ nm (full-line) is very good. When the force is increased above 0.5 pN, the curve becomes asymmetric: supercoils still form for positive coiling while local denaturation adsorbs the torsional stress for negative σ. At forces larger than 3 pN no plectonemes are observed: the torsional stress is adsorbed not by writhe but in local structural changes of the molecule.

1998). This result depends weakly on the magnitude of b which best-fitted value of $\sim$6 nm is roughly equal to twice the DNA pitch.

A number of groups have attempted to go beyond the model defined in Eq. (19) by introducing a coupling between the stretch on the double helix and its twist (Moroz and Nelson, 1998b; Marko, 1997; Nelson et al., 1997). The approach is sensible, but the comparison with the experimental data is very problematic due to the existence of structural transitions in DNA (see below) and the smallness of the predicted effect. Much theoretical work has also been done on the coupling between the intrinsic curvature and the twisting of the molecule (Schlick and Olson, 1992; Olson, 1996; Chirico and Langowski, 1996; Garrivier and Fourcade, 2000). As many regulating factors are supposed to bend the molecule, a coupling to its twist could modulate the interaction of distant sites along the DNA. This very interesting and important problem, deserves to be studied with the new tools now at our disposal. Finally, the dynamical aspects related to relaxation or transport of torsional stress along DNA (Nelson, 1999) need also to be addressed experimentally.

4.4. Torque induced transitions in DNA

The torsional buckling instability just described treats the DNA molecule as a continuous elastic tube. It ignores the underlying double-helical structure of the molecule, and its relevance is therefore limited to very low forces ($F < 0.4$ pN) or low degrees of supercoiling ($-0.015 < \sigma < 0.037$). For higher forces and degrees of supercoiling, the buildup of torque in the

molecule can be large enough to actually modify its internal structure (Strick et al., 1999). This is evidenced by breaking of the $\sigma \rightarrow -\sigma$ symmetry in the extension vs. supercoiling curves, see Fig. 8. As a critical force is reached (ipso facto a critical torque), the molecule undergoes a transition from a contracted state (plectonemic B-DNA) to a highly extended one (Strick et al., 1998). This state is characterized by the coexistence of B-DNA with denatured DNA for $\sigma < 0$ and with a new phase called P-DNA for $\sigma > 0$ (Allemand et al., 1998). This new P-DNA structure has an intrinsic degree of coiling $\sigma_p = 3$, i.e. it has 2.6 bps/turn (Allemand et al., 1998; Léger et al., 1999). Numerical simulations, supported by chemical reactivity studies, suggest that in P-DNA the phosphate backbone is winding inside the structure and the bases are exposed in solution.

These results show that at very low forces and low degrees of supercoiling DNA can locally undergo major structural transitions. These transitions might be relevant to the activity of RNA-polymerase, which is known to exert forces as high as 35 pN and to under(over)-wind the molecule up(down)-stream. It is furthermore worthwhile to notice that a structure very similar to P-DNA has apparently been observed in the packaging of DNA in the Pf1 virus. There this unusual structure is stabilised by the proteins of the virus' coat (Liu and Day, 1994).

4.5. Twisting rigidity measured through the critical torque of denaturation

The denaturation transition offers a second way to evaluate the elastic torsional persistence length C using a very simple model (Strick et al., 1999). It consists in measuring the difference in work done while stretching a single DNA molecule wound either positively or negatively by the same number of turns.

Fig. 8 shows the molecular extension as a function of supercoiling for various forces. At a low force ($F \sim 0.2$ pN) the elastic behavior of DNA is symmetric under $\sigma \rightarrow -\sigma$. Pulling on the molecule removes the writhe and thus increases the twist and the torque on the molecule. For underwound molecules (in 10 mM phosphate buffer) above the critical force ($F_c \sim 0.5$ pN) and its associated critical torque ($\Gamma_c \sim 9$ pN nm) writhing becomes energetically unfavorable. The molecule elongates, see Fig. 8 as plectonemes (which are used to absorb twist) are converted locally into melted (denatured) regions of DNA. For positive supercoilings the critical force and torque are significantly higher. Thus, we can easily find values of $|\sigma|$ such that denaturation occurs at $-|\sigma|$ whereas plectonemes remain at $|\sigma|$.

In the following, we shall use the force vs. extension measurements on DNA supercoiled by $\pm n$ turns, i.e. with the same $|\sigma|$, to estimate the torsional constant, C, the critical torque at denaturation Γ_c and the energy of denaturation per base pair (bp), ε_d.

Consider the case of a DNA of contour length l_0 at an initial extension $l_{A^+} (< l_0)$. Let us coil the molecule by $n > 0$ turns to state A^+, (Fig. 9), requiring a torsional energy T_{A^+} ($F < 0.2$ pN) and then extend it to state B^+ ($F = 4$ pN), so as to pull out its plectonemes and eliminate its writhe. Alternatively, state B^+ could be reached by first stretching the torsionally relaxed DNA and then twisting it. In that case its torsional energy T_{B^+} is purely twist. The free energy of a stretched coiled DNA being a state variable, the mechanical works performed on the molecule by stretching it from thermodynamic state A^+ to B^+ along these two different paths should be equal:

$$T_{A^+} + \Delta W_{AB^+} = T_{B^+} = \frac{C}{2l_0}(2\pi n)^2. \tag{20}$$

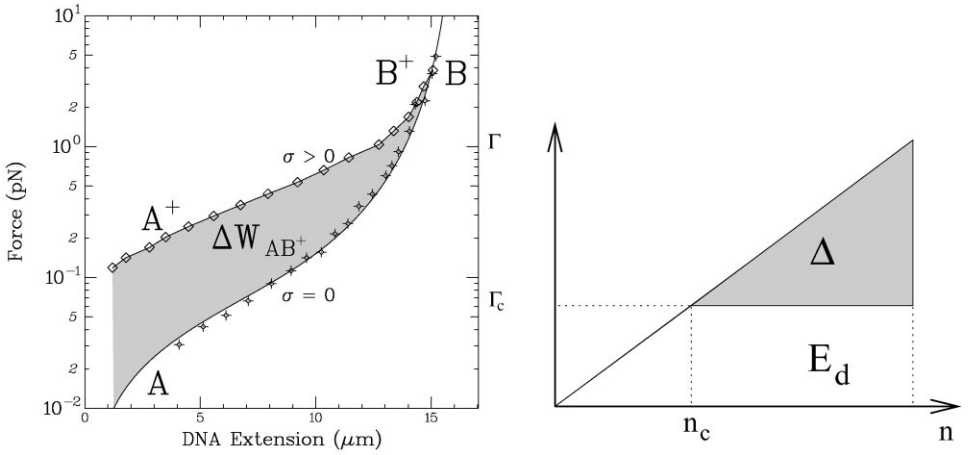

Fig. 9. LEFT: The extra work performed while stretching an overwound DNA. The molecule is overwound from points A to A^+ and then stretched along the $\sigma > 0$ curve to point B^+. The extra work performed while stretching is the shaded area between the $\sigma > 0$ and the $\sigma = 0$ curves. RIGHT dependence of the torque on the twist (number of turns). In a DNA molecule as in a twisted rod the torque increases linearly with the twist angle (number of turns). If the molecule melts because of torsional stress as expected when underwound, the torque stabilizes at a value Γ_c as it does in a rod which undergoes a torsional buckling instability. The difference Δ in the work of over and under-twisting is the shaded area shown here and in Fig. 10 left.

Here ΔW_{AB^+} is the extra work performed in stretching a coiled molecule from A^+ to B^+, the shaded area in Fig. 9. For the sake of simplicity we neglect the correction to the bare torsional constant C_0 due to the thermal fluctuations (Bouchiat and Mézard, 1998; Moroz and Nelson, 1998a). We shall see later that this approximation ($C \approx C_0$) is justified. Consider now the case in which DNA is underwound by $-n$ turns to state A^- and then stretched to state B^-. By the same reasoning as above we may write

$$T_{A^-} + \Delta W_{AB^-} = T_{B^-}. \tag{21}$$

Since when underwound the molecule partially denatures as it is pulled from A^- to B^-, the torsional energy T_{B^-} will consist of twist energy and energy of denaturation. We can nevertheless estimate T_{B^-} by considering the alternative pathway for reaching B^- by first stretching the molecule and then twisting it. In this case as the molecule is underwound, the torque Γ initially rises as in a twisted rod:

$$\Gamma = \frac{C}{l_0} 2\pi n. \tag{22}$$

When Γ reaches a critical value Γ_c after $-n_c$ turns, the molecule starts to denature. Any further increase in n enlarges the denaturation region, without affecting the torque in the molecule which stabilizes at $\Gamma = \Gamma_c$. Since mixing entropy can be neglected (Strick et al., 1998a,c; Allemand et al., 1998) the energy of denaturation is simply, see Fig. 9:

$$E_d = 2\pi(n - n_c)\Gamma_c \text{ while } T_{B^-} = \frac{C}{2l_0}(2\pi n_c)^2 + E_d. \tag{23}$$

Note that at $F \sim 4$ pN the extension of dsDNA and partially denatured DNA is the same (Allemand et al., 1998). Thus, no extra work is performed against the force when the molecule partially melts. At low force the elastic behavior of a DNA molecule is symmetric under $n \to -n$: $T_{A^+} = T_{A^-}$. Thus subtracting Eq. (21) from Eq. (20) yields

$$\Delta \equiv \Delta W_{AB^+} - \Delta W_{AB^-} = T_{B^+} - T_{B^-} = \frac{2\pi^2 C}{l_0}(n - n_c)^2, \tag{24}$$

where Δ is the measured difference between the work performed while stretching an overwound molecule and the work done while pulling on an underwound one, see shaded area in Fig. 10 (left). Plotting the value of $\sqrt{\Delta}$ vs. n, one obtains a straight line (see Fig. 10 (right)), the slope of which allows one to determine the value of the torsional constant: $C/k_BT = 86 \pm 10$ nm. The intercept of that line with the n-axis yields $n_c = 66$ turns, from which one can estimate the critical torque $\Gamma_c = 9$ pN nm and denaturation energy per bp $\varepsilon_d = E_d/10.5(n - n_c) = 1.35 k_BT$. Although the error bar on the measurement of C is still rather large, this method can be improved to yield a more precise value of C. It is nevertheless at least consistent with the current very imprecise estimate of $C/k_BT = 75 \pm 25$ nm.

We may now estimate the validity of our approximation neglecting the correction to C_0 due to the thermal fluctuations (Moroz and Nelson, 1998a). At high force these renormalize C as

$$\frac{1}{C} = \frac{1}{C_0} + \frac{k_BT}{4B\sqrt{BF}}. \tag{25}$$

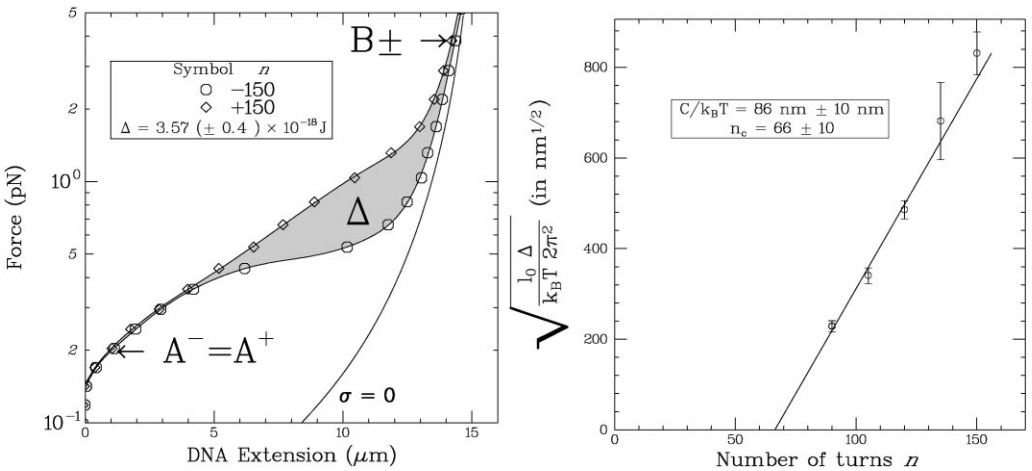

Fig. 10. LEFT: Difference in the work of stretching over and underwound DNA. (○): DNA unwound by $n = -150$ turns. (◇) DNA overwound by $n = 150$ turns. The solid curves are polynomial fits to the force-extension data. The bottom curve is the theoretical (worm-like chain) fit to the data obtained for this molecule at $\sigma = 0$: $l_0 \sim 15.7$ μm and $\xi_p = B/k_BT \sim 48$ nm (Strick et al., 1999). The shaded surface between the $\sigma > 0$ and $\sigma < 0$ curves represents the work difference Δ. In both cases, point A^+ (respectively, A^-) is reached by overwinding (underwinding) the DNA which is initially at low extension (point A, not shown). Point B^+ (B^-) is reached by stretching the molecule along the appropriate $\sigma > 0$ ($\sigma < 0$) curve. RIGHT: Plot of the square root of the work difference Δ vs. the number of turns n the molecule is over or underwound. The straight line is a best fit through the experimental points. From its slope we extract the value $C/k_BT = 86 \pm 10$ nm and from its intercept with the n-axis, $n_c = 66$ turns, we infer $\Gamma_c = 2\pi n_c C/l_0 = 9$ pN nm.

The last term on the right implies a correction of only 5% to the value of C at $F = 4\,\mathrm{pN}$, smaller than our experimental uncertainty. It is interesting to note that the value of C determined here is in good agreement with the one obtained from the measurement of the molecular extension versus σ at constant force (Bouchiat and Mézard, 1998), a totally independent measurement based on the model of a rod like chain polymer, see above.

5. DNA–protein interactions

The understanding gained on the manipulation and mechanical properties of a stretched and coiled DNA, allows one to use these measurements as a tool to probe DNA/protein interactions at the level of a single molecule, e.g. chromatin (Chatenay et al., 1997; Cui and Bustamante, 2000).

For example, the lactose repressor-mediated loop formation in a single DNA molecule was followed by studying the decrease in the Brownian motion of a DNA tethered bead (Finzi and Gelles, 1995), as its molecular leash gets shorter. Subjecting that bead to a force F should yield the free energy δG for the formation of the complex repressor/DNA. Indeed when the formation and breakdown of the loop are equiprobable: $\delta G = F\delta l$ (Marko and Siggia, 1997), where δl is the loop length.

By using the stretching force as a control parameter the polymerization of RecA on a double-stranded DNA has been induced (Léger et al., 1998; Shivashankar et al., 1999; Hegner et al., 1999). As we have seen previously, stretching a molecule with a force of $\sim$70 pN induces a transition to S-DNA, a structure of DNA presumably similar to the one adopted by the double-stranded molecule when interacting with RecA (Cluzel et al., 1996) or the TATA box-binding protein (Lebrun et al., 1997). By applying a force (even if less than 70 pN) on the molecule, one increases the probability of nucleation of an S-DNA region in the regular B-DNA helix. This S-DNA bubble has a higher affinity for RecA than B-DNA and serves as a nucleation center for the growth of a RecA fiber. As the complex RecA/DNA is about 60% longer than B-DNA, the kinetics of RecA polymerization can be followed as a function of time (at various forces) by monitoring the change in the molecular extension. Whether this stretched induced polymerization of RecA on dsDNA actually occurs in vivo remains an interesting suggestion.

The progression of an *E. coli* RNA-polymerase on a dsDNA can be followed by tethering the molecule to a small bead (Schafer et al., 1991; Yin et al., 1994) and anchoring the molecule at its other end to a RNA-pol bound to a surface. As the DNA is transcribed, the "leash" binding the bead to the surface gets shorter. The extent of its fluctuations is thus reduced and can be used to monitor the progression of the enzyme (Schafer et al., 1991). By trapping the bead with an optical tweezers, a force can be applied on a single polymerase. Its speed, pauses and the force to stall it (about 35 pN) can thus be determined (Wang et al., 1998; Yin et al., 1995).

Similarly, the replication of a single-strand DNA by a single DNA-polymerase could be observed by following the change in extension of a stretched template as a new strand is synthesized (Wuite et al., 2000; Maier et al., 2000). From the variation of the replication rate with the applied force, one could argue that a few bases (2 for T7-DNA polymerase, 4 for the Klenow fragment of polI) had to be fit between the two strands in the replication site for the enzyme to proceed. These results are in agreement with structural data and support the "induced-fit kinetic mechanism" for replication (Wong et al., 1991).

Finally, the relaxation of DNA supercoiling by a single topoisomerase (Wang, 1998) could be monitored (Strick et al., 2000) and individual enzymatic cycles observed at low ATP concentrations. From the distribution of the time intervals between successive cycles we could deduce that a single ATP was apparently burned per turnover. By averaging over many single enzymatic reactions, we could regain the kinetic behavior of topoII known from bulk measurements. Surprisingly, stretching the supercoiled DNA resulted in a lower enzymatic activity, indicating that the DNA gate religation step might be rate limiting. Finally in absence of ATP, the enzyme was observed to stabilise DNA crossovers.

These experiments open the way to a study of single mechanical enzymes, with a possibility of a detailed analysis of their cycle. Future experiments will certainly combine these manipulation techniques with single molecule observations (Kitamura et al., 1999; Harada et al., 1999; Funatsu et al., 1995; Yasuda et al., 1998) using fluorescence polarisation (Sase et al., 1997) or energy transfer (Weiss, 1999) to monitor the enzyme's structural deformation and energy consumption during its cycle.

Acknowledgements

We thank C. Bustamante, D. Chatenay, H. Clausen-Schaumann, H. Gaub, J.-F. Léger and S. Smith for sharing their data. We also thank C. Bouchiat, B. Maier, M. Mézard, for stimulating discussions.

References

Ahsan, A., Rudnick, J., Bruinsma, R., 1998. Elasticity theory of the B-DNA to S-DNA transition. Biophys. J. 74, 132–137.

Allemand, J.-F., Bensimon, D., Jullien, L., Bensimon, A., Croquette, V., 1997. pH-dependent specific binding and combing of DNA. Biophys. J. 73, 2064–2070.

Allemand, J.-F., Bensimon, D., Lavery, R., Croquette, V., 1998. Stretched and overwound DNA form a Pauling-like structure with exposed bases. Proc. Natl. Acad. Sci. USA 95, 14,152–14,157.

Amblard, F., Yurke, B., Pargellis, A., Leibler, S., 1996. A magnetic manipulator for studying local rheology and micromechanical properties of biological system. Rev. Sci. Instrum. 67 (2), 1–10.

Bensimon, A., 1996. Force: a new structural control parameter? Structure 4, 885–889.

Bensimon, D., Dohmi, D., Mézard, M., 1998. Stretching a heteropolymer. Europhys. Lett. 42, 97–102.

Bensimon, A., Simon, A.J., Chiffaudel, A., Croquette, V., Heslot, F., Bensimon, D., 1994. Alignment and sensitive detection of DNA by a moving interface. Science 265, 2096–2098.

Bensimon, D., Simon, A.J., Croquette, V., Bensimon, A., 1995. Stretching DNA with a receding meniscus: experiments and models. Phys. Rev. Lett. 74, 4754–4757.

Binder, K., Young, A.P., 1986. Spin glasses: experimental facts, theoretical concepts and open questions. Rev. Mod. Phys. 58 (4), 801–976.

Bouchiat, C., Mézard, M., 1998. Elasticity theory of a supercoiled DNA molecules. Phys. Rev. Lett. 80, 1556–1559.

Bouchiat, C., Mézard, M., 1999. Elasticity rod model of supercoiled DNA molecules. condmat/9904018.

Bouchiat, C., Wang, M.D., Block, S.M., Allemand, J.-F., Strick, T.R., Croquette, V., 1999. Estimating the persistence length of a worm-like chain molecule from force-extension measurements. Biophys. J. 76, 409–413.

Bustamante, C., Marko, J.F., Siggia, E.D., Smith, S., 1994. Entropic elasticity of λ-phage DNA. Science 265, 1599–1600.

Cantor, C.R., Schimmel, P.R., 1980. Biophysical Chemistry, Part III: The Behaviour of Biological Macromolecules. W.H. Freemann, San Francisco.
Chatenay, D., Houchmanzadeh, B., Marko, J.F., Libchaber, A., 1997. Elasticity and structure of eukaryote chromosomes studied by micromanipulation and micropipette aspiration. J. Cell. Biol. 139, 1–12.
Chee, M., Yang, R., Hubbell, E., Berno, A., Huang, X.C., Stern, D., Winkler, J., Lockhart, D.J., Morris, M.S., Fodor, S.P.A., 1996. Accessing genetic information with high-density DNA arrays. Science 274, 610–614.
Chirico, G., Langowski, J., 1996. Brownian dynamics simulations of supercoiled DNA with bent sequences. Biophys. J. 71, 955–971.
Chu, S., 1991. Laser manipulation of atoms and particles. Science 253, 861–866.
Cizeau, P., Viovy, J.L., 1997. Modeling extreme extension of DNA. Biopolymers 42, 383–385.
Cluzel, P., Lebrun, A., Heller, C., Lavery, R., Viovy, J.-L., Chatenay, D., Caron, F., 1996. DNA: an extensible molecule. Science 271, 792–794.
Cui, Y., Bustamante, C., 2000. Pulling a single chromatin fiber reveals the forces that maintain its higher order structure. Proc. Natl. Acad. Sci. (USA) 97, 127–132.
de Gennes, P.G., 1979. Scaling concepts in Polymer Physics. Cornell University Press, Ithaca.
Einstein, A., 1956. Investigation of the Brownian Theory of Movement. Dover Publication, New York.
Engel, A., Gaub, H.E., Müller, D.J., 1999. Atomic force microscopy: a forceful way with single molecules. Curr. Biol. 9, R133–R136.
Essevaz-Roulet, B., Bockelmann, U., Heslot, F., 1997. Mechanical separation of the complementary strands of DNA. Proc. Natl. Acad. Sci. (USA) 94, 11,935–11,940.
Finer, J.T., Simmons, R.M., Spudich, J.A., 1994. Single myosin molecule mechanics: piconewton forces and nanometre steps. Nature 368, 113–119.
Finzi, L., Gelles, J., 1995. Measurement of lactose repressor-mediated loop formation and breakdown in single DNA molecules. Science 267, 378–380.
Fisher, M.E., 1964. Magnetism in one-dimensional systems — the Heisenberg model for infinite spin. Am. J. Phys. 32, 343–346.
Fixman, M., Kovac, J., 1973. Polymer conformational statistics III: modified Gaussian models of the stiff chains. J. Chem. Phys. 58, 1564–1568.
Florin, E.L., Moy, V.T., Gaub, H.E., 1994. Adhesion force between individual ligand–receptor pairs. Science 264, 415–417.
Flory, P., 1975. Principles of Polymer Chemistry. Cornell University Press, Ithaca.
Forterre, P., 1996. A hot topic: the origin of hyperthermophiles (minireview). Cell 85, 789–792.
Funatsu, T., Harada, Y., Tokunaga, M., Saito, K., Yanagida, T., 1995. Imaging of single fluorescent molecules and individual ATP turnovers by single myosin molecules in aqueous solution. Nature 374, 555–559.
Garrivier, D., Fourcade, B., 2000. Twisting DNA with variable intrinsic curvature. Europhys. Lett. 49, 390–395.
Gosse, C., Croquette, V., 1999. Magnetic tweezers. Rev. Sci. Instrum., in preparation.
Hagerman, P.J., 1988. Flexibility of DNA. Ann. Rev. Biophys. Chem. 17, 265–268.
Harada, Y., Funatsu, T., Murakami, K., Nonoyama, Y., Ishihama, A., Yanagida, T., 1999. Single-molecule imaging of RNA polymerase-DNA interactions in real time. Biophys. J. 76, 709–715.
Hegner, M., Smith, S.B., Bustamante, C., 1999. Polymerization and mechanical properties of single RecA-DNA filaments. Proc. Natl. Acad. Sci. USA 96, 10,109–10,114.
Hogan, M.E., Austin, R.H., 1987. Importance of DNA stiffness in protein-DNA binding specificity. Nature 329, 263–266.
Hua, W., Young, E.C., Fleming, M.L., Gelles, J., 1997. Coupling of kinesin steps to ATP hydrolysis. Nature 388, 390–393.
Ishijima, A., Doi, T., Sakurada, K., Yanagida, T., 1991. Sub-piconewtown force fluctuations of actomyosin in vitro. Nature 352, 301–306.
Kellermayer, M.S.Z., Smith, S.B., Granzier, H.L., Bustamante, C., 1997. Folding–unfolding transition in single titin molecules characterized with laser tweezers. Science 276, 1112–1116.
Kikuchi, A., Asai, K., 1984. Reverse-gyrase — a topoisomerase which introduces positive superhelical turns into DNA. Nature 309, 677–681.

Kitamura, K., Tokunaga, M., Iwane, A.H., Yanagida, T., 1999. A single myosin head moves along an actin filament with regular steps of 5.3 nanometers. Nature 397, 129–134.
Lebrun, A., Lavery, R., 1996. Modelling extreme deformations of DNA. Nucl. Acids Res. 24, 2260.
Lebrun, A., Lavery, R., 1997. Unusual DNA conformations. Curr. Op. Struct. Biol. 7, 348–354.
Lebrun, A., Shakked, Z., Lavery, R., 1997. Local DNA stretching mimics the distortion caused by the TATA box-binding protein. Proc. Natl. Acad. Sci. USA 94, 2993–2998.
Léger, J.F., Robert, J., Bourdieu, L., Chatenay, D., Marko, J.F., 1998. RecA binding to a single double-stranded DNA molecule: a possible role of DNA conformational fluctuations. Proc. Natl. Acad. Sci. USA 95, 12,295–12,296.
Léger, J.F., Romano, G., Sarkar, A., Robert, J., Bourdieu, L., Chatenay, D., Marko, J.F., 1999. Structural transitions of a twisted and stretched DNA molecule. Phys. Rev. Lett. 83, 1066–1069.
Liu, D.J., Day, L.A., 1994. Pf1 virus structure: helical coat protein and DNA with paraxial phosphates. Science 265, 671–674.
Liu, L.F., Wang, J.C., 1987. Supercoiling of the DNA template during transcription. Proc. Natl. Acad. Sci. USA 84, 7024–7027.
Maier, B., Bensimon, D., Croquette, V., 2000. Replication by a single DNA-polymerase of a stretched single strand DNA. Proc. Natl. Acad. Sci. USA, accepted for publication.
Marko, J.F., 1997. Stretching must twist DNA. Europhys. Lett. 38, 183–188.
Marko, J.F., 1998. DNA under high tension: overstreching undertwisting and relaxation dynamics. Phys. Rev. E 57 (2), 2134–2149.
Marko, J.F., Siggia, E., 1995a. Statistical mechanics of supercoiled DNA. Phys. Rev. E 52 (3), 2912–2938.
Marko, J.F., Siggia, E., 1995b. Stretching DNA. Macromolecules 28 (26), 8759–8770.
Marko, J.F., Siggia, E.D., 1997. Driving proteins off DNA using applied tension. Biophys. J. 73, 2173–2178.
Moroz, J.D., Nelson, P., 1998a. Torsional directed walks, entropic elasticity and DNA twist stiffness. Proc. Natl. Acad. Sci (USA) 94, 14,418–14,422.
Moroz, J.D., Nelson, P., 1998b. Entropic elasticity of twist-storing polymers. Macromolecules 31, 6333–6347.
Michalet, X., Ekong, R., Fougerousse, F., Rousseaux, S., Schurra, C., Povey, S., Beckmann, J.S., Bensimon, A, 1997. Dynamic molecular combing: stretching the whole human genome for high resolution studies. Science 277, 1518–1523.
Nelson, P., 1998. Sequence-disorder effects on DNA entropic elasticity. Phys. Rev. Lett. 80, 5810–5812.
Nelson, P., 1999. Transport of torsional stress in DNA. Proc. Natl. Acad. Sci. 96, 14,342–14,347.
Nelson, P., Kamien, R.D., Lubensky, T.C., O'Hern, C.S., 1997. Direct determination of DNA twist-stretch coupling. Europhys. Lett. 38, 237–242.
Olson, W.K., 1996. Simulating DNA at low resolution. Curr. Op. Struct. Biol. 6, 242–256.
Perkins, T.T., Smith, D.E., Chu, S., 1994a. Direct observation of tube-like motion of a single polymer chain. Science 264, 819–822.
Perkins, T.T., Quake, S.R., Smith, D.E., Chu, S., 1994b. Relaxation of a single DNA molecule observed by optical microscopy. Science 264, 822–826.
Reif, F., 1965. Fundamentals of Statistical and Thermal Physics. McGraw-Hill, New York.
Rief, M., Clausen-Schaumann, H., Gaub, H.E., 1999. Sequence-dependent mechanics of single DNA molecules. Nature Struct. Bio. 6, 346–349.
Rief, M., Gautel, M., Oesterhelt, F., Fernandez, J.M., Gaub, H.E., 1997. Reversible unfolding of individual titin immunoglobulin domains by AFM. Science 276, 1109–1112.
Saito, K., Takaaki Aoki, Toshiaki Aoki, Yanagida, T., 1994. Movement of single myosin filaments and myosin step size on an actin filament suspended in solution by a laser trap. Biophys. J. 66, 769–777.
Sano, T., Smith, C.L., Cantor, C.R., 1992. Immuno-PCR: very sensitive antigen detection by means of specific antibody-DNA conjugates. Science 258, 120–122.
Sase, I., Miyata, H., Ishiwata, S., Kinosita, K., 1997. Axial rotation of sliding actin filaments revealed by single-fluorophore imaging. Proc. Natl. Acad. Sci. USA 94, 5646–5650.
Schafer, D.A., Gelles, J., Sheetz, M.P., Landick, R., 1991. Transcription by single molecules of RNA polymerase observed by light microscopy. Nature 352, 444–448.

Schellman, J.A., Harvey, S.C., 1995. Static contributions to the persistence length of DNA and dynamic contributions to DNA curvature. Biophys. Chem. 55, 95–114.
Schlick, T., Olson, W.K., 1992. Supercoiled DNA energetics and dynamics by computer simulation. J. Mol. Biol. 223, 1089–1119.
Schnitzer, M.J., Block, S.M., 1997. Kinesin hydrolyses one ATP per 8-nm step. Nature 388, 386–390.
Shivashankar, G.V., Feingold, M., Kritchevsky, O., Libchaber, A., 1999. RecA polymerization on double-stranded DNA by using single-molecule manipulation: the role of ATP hydrolysis. Proc. Natl. Acad. Sci. USA 96, 7916–7921.
Simmons, R.M., Finer, J.T., Chu, S., Spudich, J.A., 1996. Quantitative measurements of force and displacement using an optical trap. Biophys. J. 70, 1813–1822.
Smith, S.B., 1998. Stretch transitions observed in single biopolymer molecules (DNA or protein) using laser tweezers. Thesis, U. Twente, Netherlands.
Smith, S.B., Cui, Y., Bustamante, C., 1996. Overstretching B-DNA: the elastic response of individual double-stranded and single-stranded DNA molecules. Science 271, 795–799.
Smith, S.B., Finzi, L., Bustamante, C., 1992. Direct mechanical measurements of the elasticity of single DNA molecules by using magnetic beads. Science 258, 1122–1126.
Stasiak, A., Di Capua, E., 1982. The helicity of DNA in complexes with Rec-A protein. Nature 299, 185–187.
Stasiak, A., Di Capua, E., Koller, T., 1983. Unwinding of duplex DNA in complexes with Rec-A protein. Cold Spring Harbor Symposium on Quantitative Biology, Vol. 47, pp. 811–820.
Strick, T., Allemand, J.F., Bensimon, D., Bensimon, A., Croquette, V., 1996. The elasticity of a single supercoiled DNA molecule. Science 271, 1835–1837.
Strick, T., Allemand, J.-F., Bensimon, D., Croquette, V., 1998a. The behavior of supercoiled DNA. Biophys. J. 74, 2016–2028.
Strick, T., Allemand, J.-F., Croquette, V., Bensimon, D., 1998b. Physical approaches to the study of DNA. J. Stat. Phys. 93, 647–672.
Strick, T., Croquette, V., Bensimon, D., 1998c. Homologous pairing in streched supercoiled DNA. Proc. Natl. Acad. Sci. (USA) 95, 10,579–10,583.
Strick, T., Allemand, J.-F., Bensimon, D., Lavery, R., Croquette, V., 1999. Phase coexistence in a single DNA molecule. Physica A 263, 392–404.
Strick, T., Bensimon, D., Croquette, V., 1999. Micro-mechanical measurement of the torsional modulus of DNA. Genetica, Proceedings of NATO ARW on Structural Biology and Functional Genomics, 1998, Vol. 106, pp. 57–62.
Strick, T.R., Croquette, V., Bensimon, D., 2000. Single-molecule analysis of DNA uncoiling by a type II topoisomerase. Nature 404, 901–904.
Trifonov, E.N., Tan, R.K.-Z., Harvey, S.C., 1987. Static Persistence Length of DNA. Adenine Press.
Vologodskii, A.V., 1994. DNA extension under the action of an external force. Macromolecules 27, 5623–5625.
Vologodskii, A., Marko, J.F., 1997. Extension of torsionally stressed DNA by external force. Biophys. J. 73, 123–132.
Wang, J.C., 1998. Moving one DNA double helix through another by a type II DNA topoisomerase: the story of a simple molecular machine. Quart. Rev. Biophys. 31, 107–144.
Wang, M.D., Schnitzer, M.J., Yin, H., Landick, R., Gelles, J., Block, S., 1998. Force and velocity measured for single molecules of RNA polymerase. Science 282, 902–907.
Wang, M.D., Yin, H., Landick, R., Gelles, J., Block, S., 1997. Stretching DNA with optical tweezers. Biophys. J. 72, 1335–1346.
Weier, H.-U.G., Wang, M., Mullikin, J.C., Zhu, Y., Cheng, J.-F., Greulich, K.M., Bensimon, A., Gray, J.M., 1995. Quantitative DNA fiber mapping. Human Mol. Gen. 4, 1903–1910.
Weiss, S., 1999. Fluorescence spectroscopy of single biomolecules. Science 283, 1676–1683.
White, J.H., 1969. Self linking and the gauss integral in higher dimensions. Am. J. Math. 91, 693–728.
Wilkins, M.H.F., Gosling, R.G., Seeds, W.E., 1951. Nucleic acid: an extensible molecule? Nature 167, 759–760.
Woese, C.R., Fox, G.E., 1977. Phylogenetic structure of the prokaryotic domain: the primary kingdoms. Proc. Natl. Acad. Sci. USA 74, 5088–5090.
Woese, C.R., Kandler, O., Wheelis, M.L., 1990. Towards a natural system of organisms: proposal for the domain: archaea, bacteria and eucarya. Proc. Natl. Acad. Sci. USA 87, 4576–4579.

Wong, I., Patel, S.S., Johnson, K.A., 1991. An induced-fit kinetic mechanism for DNA replication fidelity: direct measurement by single-turnover kinetics. Biochemistry 30, 526–537.

Wuite, G.J.L., Smith, S.B., Young, M., Keller, D., Bustamante, C., 2000. Single-molecule studies of the effect of template tension on T7 DNA polymerase activity. Nature 404, 103–106.

Yasuda, R., Noji, H., Kinosita, K., Yoshida, M., 1998. F_1-ATPase is a highly efficient molecular motor that rotates with discrete 120° steps. Cell 93, 1117–1124.

Yin, H., Landick, R., Gelles, J., 1994. Tethered particle motion method for studying transcript elongation by a single RNA polymerase molecule. Biophys. J. 67, 2468–2478.

Yin, H., Wang, M.D., Svoboda, K., Landick, R., Block, S., Gelles, J., 1995. Transcription against a applied force. Science 270, 1653–1657.